Written Article Assessment
ME520: Heat Conduction
May 12, 2017

ME 520 Final Paper, Spring 2017
A Review and Numerical Model for the *3ω method for specific heat and thermal conductivity measurements*, by Lu, Yi, and Zhang (2001).

Josh Stout

ABSTRACT

The core assumptions and analyses behind the 3ω thermal property measurement technique proposed by Lu, Yi, and Yang [1] are examined and found to be reasonable. Their application of this 3ω model to a platinum wire and bundle of carbon nanotubes is also inspected, and found to be defendable for the platinum sample and potentially misleading for the carbon nanotubes.

For demonstration of this method in a numerical system with controllable radiative heat losses, a finite volume model is built. This complete 1D model is shown to be in very good agreement with the analytical model as provided by Lu et al., including the thermal property correction required to compensate for the radiative losses.

INTRODUCTION

Importance

The article under review is important for both experimental and numerical heat conduction problems. The analytical model presented provides the theory for a high accuracy measurement technique. This method may be particularly attractive for material samples that may otherwise not be experimentally tractable, due to measurement noise from more traditional means. This could be due to the mass or length scales involved, as may be the case for the bundle of carbon nanotubes that Lu examined.

Many other works have built upon or made use of this article since its publication; recent applications often revolve around the analytical groundwork and apply it to modern material measurements. Common themes among these are suspended nanofilms [2], nanowires [3], carbon nanotube fibers [4], and nano thermocouples [5].

The 3ω Paper

Lu first outlines some of the previous work done on 3ω measurement techniques, starting with Corbino's initial observation that the temperature fluctuation in an ac heated wire can provide some insight to the thermal properties for the wire's material [6]. Lu moves on to state that the subsequent investigations for the general 3ω method since the 1960's have allowed the method to become practical, but that the analytical solutions of the heat conduction equation were only provided for the limits of high and low frequency.

A new analytical solution for 1D heat conduction, driven by a periodic volumetric heat generation representing the ac current is then derived. The solution is obtained through a temperature offset to homogenize boundary conditions, an implementation of the impulse theorem, and the assumption that heating power inhomogeneity due to the temperature dependence of electrical resistance is small in comparison to the total heating power. The temperature solution is then used to calculate an average electrical resistance fluctuation across the domain, allowing for the calculation of a V_{rms} curve as a function of driving frequency. The 3ω component of this V_{rms}, is then isolated and shown to contain information on both the thermal conductivity and thermal time constant of the specimen, and therefore the specific heat.

This general solution for $V_{3\omega,rms}$ is then compared to the previously obtained solutions for the high and low frequency limits and found to match exactly. Furthermore, it is shown how each of these limits only contains information for either the thermal conductivity or specific heat, demonstrating the advantage of the general solution.

Following this, various sources of error are considered. The first of which is that due to truncation of the Fourier expansion terms in $V_{3\omega,rms}$. It is shown that for low frequencies in the range of $0 < 2\omega\gamma < 10$, the truncation error is very nearly constant, allowing for an improved solution fit through a slight shift. This is then stated to result in fitted thermal conductivity, thermal time constant, and specific heat values that vary by less than 0.1% from those obtained with the non-truncated equation.

The next source of error is that which may be introduced through the experimental setup in the form of radial heat loss. Ultimately, it is found that the equation solution forms do not particularly change, except that the thermal conductivity and thermal time constant are replaced by "apparent" values, which vary from the true values by a factor related to the magnitude of this extra heat loss. This introduces a new condition showing that radial heat transfer can be neglected if the product of this heat loss coefficient and the thermal time constant is much less than 1. This can also be interpreted as the resulting radial power being much less than the axial heat current. Regardless, they also show that even when information regarding radial losses from the sample is missing, the true value for specific heat is retained, and only the true value of thermal conductivity is lost. This analyses of course applies to both radiative and convective losses, although convective losses are more easily avoided through the use of a high vacuum.

With the analytical groundwork and error consideration out of the way, Lu moves on to present an experimental setup with results. The two materials considered are platinum wires and bundles of multiwall carbon nanotubes, which differ in the sign of their electrical resistance temperature coefficients. For both cases, they observe the appropriate relationship between $V_{3\omega,rms}$ with current, and $V_{3\omega,rms}$ with frequency. It is also

pointed out that due to the 3ω voltage being buried within the 1ω voltage, special care needs to be taken with how the 3ω signal is extracted. If the signal is too small to measure, it may be increased through either an increased driving current or a change in the geometry of the specimen, though they warn that increasing the current in particular can lead to the violation of several previously outlined assumptions.

After collecting data from both materials over an appropriate current amplitude and frequency range, the thermal conductivity, diffusivity, and specific heat for the platinum sample are found to agree well with the standard values. The observed peak for thermal conductivity at low temperatures is less pronounced than the standard for a perfect sample, but the discrepancy is accredited to the experimental sample containing some number of defects more than the standard sample.

As for the experimental influence of radiative and convective heat losses, convection is tested through varying the high vacuum pressure. It was found that changing this vacuum pressure by a factor of two did not result in a different thermal conductivity, so the influence of convection was determined to be negligible. The insensitivity of specific heat is also tested by destroying the vacuum in another experimental run. In both cases, the worst-case estimated radiative heat coefficient is determined to be small enough that radiative heat transfer is negligible.

For the carbon nanotube bundle, it is reasoned that although the material is highly anisotropic, the 1D solution may still be applied due to the relative thermal time constants in the radial and axial directions. The experimental $V_{3\omega,rms}$ data is found to have the predicted dependence on current frequency and amplitude, leading to the conclusion that the resulting thermal conductivity and specific heat are accurate. Similarly to the platinum case, estimates for radial heat radiation are found to be effectively negligible.

Lu concludes that this model for determining the thermal conductivity and specific heat of rod or filament-like samples is good for within 2-4 %, and that the presence of radial heat conduction will result in an apparent thermal conductivity higher than reality, but an unaffected specific heat.

Advantages & Disadvantages

The advantages of this method primarily revolve around the simultaneous measurement of thermal conductivity and specific heat, in addition to the related quantities, thermal time constant and thermal diffusivity. It is also desirable in that the test specimen itself is used to produce the necessary heating, and the influence of radiative heat conduction are well understood and minimizable. As a result, the specimen sizes may also be very small so long as the necessary assumptions are met, as illustrated by the measurement of the 10^{-9}g carbon nanotube sample.

As a side effect of these advantages, there were some necessary assumptions made for the model that may not be desirable in an experimental setting. Depending on the material, there may be some limits placed on the appropriate current frequency that are not practical, or the relative dimensions of the desired measurement material may be inconvenient. The fit for the model also requires that some electrical material properties be known ahead of time, such as the electrical resistance and the electrical resistance temperature coefficient. While these should be obtainable with the same experimental setup, it may still be undesirable. This also of course means that if a sample is not electrically conductive, then this method is not suitable.

In contrast, a steady state method such as the Searle's bar method [7] only measures the thermal conductivity, and is a relatively complicated setup that requires an external heater, water cooling system, and sufficient specimen dimensions to avoid heat flow interference from the thermocouples.

Another method, as outlined by Riegel and Weber [8], presents the calculation of specific heat through the use of a calorimeter and analysis of the temperature time response for the sample. As presented, this method is only for very low temperatures (0.2-4.5 K), and requires a much longer experimental duration due to the requirement of sample equilibrium.

ANALYTICAL SOLUTION AND VALIDATION

Review of Model

As presented by Lu, the governing equation is as follows:

$$\rho C_P \frac{\partial}{\partial t} T\left(x,t\right) - \kappa \frac{\partial^2}{\partial x^2} T\left(x,t\right) = \frac{I_0^2 \sin\left(\omega t\right)^2}{LS} \left[R + R'\left(T\left(x,t\right) - T_0\right)\right] \quad (1)$$

With fixed boundary conditions according to:

$$T(0,t) = T_0 \quad (2)$$

$$T(L,t) = T_0 \quad (3)$$

$$T(x, -\infty) = T_0 \quad (4)$$

I_0 is the driving current amplitude, L is the sample length, and S is the sample cross-section area. The equation and boundary conditions are then somewhat simplified by defining a new $\Delta(x,t) = T(x,t) - T_0$ such that the variation in temperature from the initial value is considered, rather than the absolute.

By invoking the impulse theorem, a new function, z(x,;τ), is defined by and satisfies the following 2 equations:

$$\Delta(x,t) = \int_{-\infty}^{t} z(x,t;\tau) d\tau \quad (5)$$

$$\frac{\partial z}{\partial t} - \alpha \frac{\partial^2 z}{\partial x^2} - c \sin^2\left(\omega t z\right) = 0 \quad (6)$$

By then considering z as a spatial Fourier series according to:

$$z(x,t;\tau) = \sum_{n=1}^{\infty} U_n(t;\tau) \sin\left(\frac{n\pi x}{L}\right) \quad (7)$$

and plugging this definition into Eq. (6), the first major assumption is approached. This is that $n^2\pi^2\alpha/L^2 \gg c$, where $c = I_0^2 R'/\rho C_P LS$, resulting in the previously cited requirement that the heating power inhomogeneity from the resistance temperature coefficient be much smaller than the total heat, or capacity for axial heat transfer. This makes good physical sense for most relevant experimental systems, as we would expect that for conductive materials undergoing small temperature changes,

any local temperature variation due to a small electrical resistance fluctuation would smooth out much faster than the overall temperature response.

Following this, if the c term is dropped due to the above assumption, the ODE for $U_n(t;\tau)$ can be directly solved and back substituted through to find the analytical solution for $\Delta(x,t)$. Of course, the heat source term is responsible for much of this necessary manipulation, as without it, the governing equation would simply be a parabolic PDE that can be solved a number of other ways, such as separation of variables.

Once the temperature solution is known, an equation for the average electrical resistance fluctuation over the domain can be simply calculated. This electrical resistance fluctuation equation multiplied with the input current produces the term containing 3ω time response, which can then be converted into a steady root mean squared value as a function of input frequency. This solution is still present as an infinite sum however, so a decision on how many terms to truncate must be made. As shown by Lu, sufficient accuracy for most cases (roughly 2-4 %) can be obtained by only considering the first term of this sum, with a corrective term available for even greater accuracy.

This RMS solution without the corrective term is:

$$V_{3\omega}(t) \approx \frac{4I^3 LRR'}{\pi^4 \kappa S \sqrt{1+(2\omega\gamma)^2}} \tag{8}$$

where I is now the RMS value of the driving current. As this is the only term in the solution that results from the 3ω time dependence, if this signal is can to be experimentally isolated, then this equation form can be used to predict the 3ω response for any given input frequency

While the procedure for obtaining the $V_{3\omega}$ equation from the temperature solution is fairly set, it may be possible to obtain the temperature solution with another method, such as Duhamel's method. The main trick is of course that the source term is explicitly time dependent and introduces a linear term in temperature. The same argument would need to be made for the relative magnitudes of temperature inhomogeneity and axial heat flow, however.

Description of Time Evolution

For the physicality of high and low frequency voltage limits, interpretation is fairly straight forward. For the very low frequency, the phase offset between the current and temperature solution disappears, such that every peak or trough in the current occurs at the same moment as the greatest rate of increase in temperature, and similarly every 0 point in current corresponds to the fastest rate of decrease in temperature. The 3ω voltage is instead offset by exactly $\pi/2$. Both of these can then be interpreted as the material's heat capacity dropping in importance relative to the thermal conduction, as reflected by the 3ω voltage solution only depending on thermal conductivity.

On the other end of the spectrum, when the load frequency approaches infinity the timescale associated with the current oscillations becomes much faster than the timescale associated with heat diffusion. This results in the heat load becoming effectively steady on the timescale of heat diffusion. This causes the temperature solution to no longer oscillate in time and appear as the solution for an applied dc load. This may result in the 3ω voltage solution shrinking in amplitude, but it now only depends on the material's specific heat, or how quickly the material can react to the rapid changes in heat load.

Review of the Experimental

Experimental results were presented using this 3ω approach for both platinum and carbon nanotubes.

First and foremost, the results depend upon the validity of Fourier heat conduction for the system. One way to check this is to compare the scale of the mean free path for each carrier type to the scale of the sample. The platinum wire is stated as having a diameter of 20 μm and length of 8 mm. The fcc unit cell for a platinum crystal is on the order of 0.4 nm, which is 4 orders of magnitude smaller than the smallest wire dimension. It is generally expected that the mean free path for both phonons and photons is of a similar scale to the atomic, so heat diffusion should be well represented by a continuum. Though for very low temperatures, caution should be taken for the growing mean free path of phonons in a perfect lattice. This ties into the results presented by Lu, in that the calculated thermal conduction at low temperatures is smaller than that of the perfect standard platinum. This is attributed to possible impurities in composition or crystal structure, which is consistent with the idea of imperfections dominating the mean free path of phonons at low temperatures. This is also seen in the Wiedemann-Franz ratio; for small temperatures, the ratio of thermal conductivity from electrons to electron conductivity is expected to approach 0. As this is not the case, the thermal conductivity at low temperatures must have some component related to the phonons, which is then governed by the presence of defects.

As for the carbon nanotube results, Lu's assertion that the thermal time constant in the radial direction is much shorter than in the axial direction is perhaps debatable. While it is true that the dimensional scale favors this, Lu also states that the thermal conductivity itself is highly anisotropic, with high conduction in the axial direction. If the ratio of time constants for the radial and axial directions is examined, the following results:

$$\frac{\gamma_{rad}}{\gamma_{ax}} = \frac{R^2 \rho C_P}{\pi^2 \kappa_{rad}} \frac{\pi^2 \kappa_{ax}}{L^2 \rho C_P} = \frac{\kappa_{ax} R^2}{\kappa_{rad} L^2} \tag{9}$$

This could leave us to believe that if the ratio of axial to radial thermal conductivities is similar in scale to the squared ratio of wire length to radius, then the above timescale argument may not be true. On the other hand, for a bundle of tubes, heat only needs to travel in the cross-plane direction once every tube diameter's distance; the rest of the conduction path will be along the surface of the tubes. This means that a more appropriate conduction length would be strongly related to either the number of tube-tube interfaces, or the diameter of an individual tube, both of which are much shorter than the total wire diameter.

If it is accepted that the above argument is true for the particular sample under test, then the resulting thermal values should be valid. This being said, there may be more subtleties in the structure of any one particular sample of nanotubes that could prove misleading for this result, particularly with respect to the behavior of a single tube. Presumably, for conduction along a single tube, the electrons may conduct heat along either the inner or outer surfaces. In a bundle of tubes, depending on how they are packed, there may be electron paths on the outside surface

that become restricted due to contacting neighboring surfaces. Additionally, when an individual tube breaks, that is the end of that tube. In a bundle, individual tubes may be completely broken while neighboring tubes are not. Any complete breaks in the axial direction could have a fairly significant influence in the overall conduction of a bundle, particularly if the current is not uniformly initialized across the cross section.

Review of Key Findings

The key findings of Lu primarily relate to the solution of the 1D analytical model. By solving the equation with a general load frequency and using minimal assumptions, the resulting predictive equations are shown to be accurate for two materials that are fundamentally different in structure with opposite dependencies of electrical resistance on temperature. It is also important for the robustness of the model that error introduced from non-conductive heat losses can either be accounted for or shown to be small.

These things have allowed the model to be used for the analysis of many more materials. Li et al. use and extend this 3ω model to the measurement of thermal properties for a 40nm thick platinum film, over a temperature range of 80 to 380 K [2]. Meng et al. were examining and optimizing the thermal management of individual SnO_2 nanowires, which requires intimate knowledge of the wire's thermal properties. They were able to utilize this 3ω method to suitably calculate the thermal properties for their $\sim$79nm diameter wires [3]. Qiu et al. expand upon the carbon nanotube bundle measurements and study a method of improving the conduction of inter-bundle interfaces. They use this method for documenting the thermal properties as a function of bundle length [4].

RESULTS AND DISCUSSION

For a 1D numerical model, the following equation including radiative loss and current heating will be integrated over time and space according to a simple finite volume method:

$$\frac{\partial T}{\partial t} - \alpha\frac{\partial^2 T}{\partial x^2} = h\sin(\omega t)^2\left[R + R'T\right] - \frac{4\epsilon\sigma\left[T^4 + 4T^3T_0 + 6T^2T_0^2 + 4TT_0^3\right]}{D} \quad (10)$$

Where T is now defined as the variation in temperature from T_0, and the new constant h is defined as $I_0^2/LS\rho C_P$, ϵ is radiative emissivity, and σ is the Stefan-Boltzmann constant.

In order to incorporate a heat generation term as a function of the dependent variable, an iterative timestep procedure will be utilized, where G will be used to encapsulate and linearize everything on the right side of Eq. 10.

Discretizing this results in the center-cell equation with time as superscript and space as subscript:

$$T_i^{j+1} - T_i^j = \frac{\alpha\Delta t}{\Delta x^2}\left(T_{i+1}^j - 2T_i^j + T_{j-1}^j\right) + \Delta t\left[G^* + \frac{\partial G^*}{\partial T}\left(T_i^{j+1} - T_i^*\right)\right] \quad (11)$$

$$T_i^{j+1} = \frac{1}{1-\Delta t\frac{\partial G^*}{\partial T}}\left[T_i^j + \frac{\alpha\Delta t}{\Delta x^2}\left(T_{i+1}^j - 2T_i^j + T_{j-1}^j\right)\right] + \frac{1}{1-\Delta t\frac{\partial G^*}{\partial T}}\left[\Delta t\left(G^* - \frac{\partial G^*}{\partial T}T_i^*\right)\right] \quad (12)$$

Where * indicates the iteration's best guess value, starting from the solution to the previous timestep and updating to the most recent T^{j+1} value. The boundary cell equations need only be slightly modified to include the Dirichlet boundary condition for 0 in the temperature variation variable.

As this is effectively an explicit FTCS scheme, the spatial domain is composed of 25 uniform cells, and the timestep size is chosen according to Von Neumann FTCS stability: $\Delta t = \Delta x^2/2\alpha$.

Once a steadily oscillating temperature solution is obtained, the electrical resistance fluctuation as a function of time is numerically evaluated according to:

$$\delta R = \frac{R'}{L}\int_0^L T\,dx \quad (13)$$

This is then added to the reference resistance and multiplied by the driving current in order to obtain the full voltage response. Then, due to the orthogonality of 1ω and 3ω sine functions, the 3ω component can be isolated by using Python's non-linear least squares optimizer to fit a 3ω sine function of unknown amplitude and phase to the data. Note that for numerical reasons, 3ω response was actually obtained by first subtracting out the best fit 1ω response and then finding the best fit for 3ω. The RMS of this 3ω voltage can then be calculated for the given input frequency.

This process may be repeated over a range of frequencies, such that the resulting data points may then be fit to the expected functional form of $V_{3\omega,rms}$ and the thermal conductivity and specific heat may be re-extracted. These can then of course be directly compared to the values used in the model input.

For simplicity's sake, the following material properties and constants are chosen for the numerical model:

$$\kappa = 10\ W/mK \quad \rho = 1\ kg/m^3 \quad C_P = 1\ J/kgK$$
$$R = 400\ \Omega \quad R' = 10^{-1}\ \Omega/K \quad I_0 = 10^{-1}\ A$$
$$L = 1\ m \quad D = 10^{-1}\ m$$
$$\epsilon = 1 \quad T_0 = 275\ K$$

These result in $\alpha = 10$ and $\gamma = 1/10\pi^2$, and an appropriate input frequency range of $0 < \omega < 20\pi^2$.

These parameter satisfy the condition that heating power inhomogeneity from the resistance fluctuation is less than the axial heat conduction capacity, but do not satisfy the condition for radiation being negligible. This should allow for an observable and predictable difference between the input parameters and the output "apparent" parameters. A reference case with $T_0 = 0$ will also be run as a reference point for the minimum influence of radiative heat transfer.

While the simulation results behave as expected overall, the resulting thermal conductivity and specific heat values were coming out larger than expected by a factor of 3. This could be explained by a factor of 3 error in the 3ω RMS voltage, but I have not been able to identify where an isolated mistake could

have taken place. If I correct voltage by this factor of 3, the results match up extremely well.

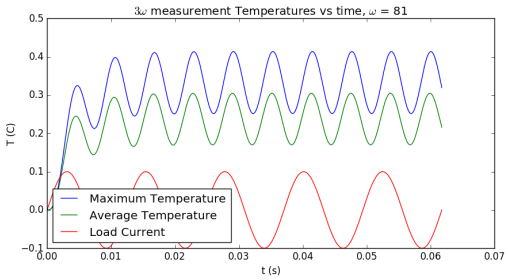

Figure 1: Temperatures vs Time for $\omega = 81$ Hz, with 275K ambient

In order to demonstrate that the time interval over which measurement was taken is representative of the oscillatory steady state, Fig. 1 shows the time response of maximum temperature and average temperature alongside the driving current for the highest frequency considered. Starting from an initial temperature variation of T = 0, the system appears to have reached its steady condition by the end of the second current oscillation. In order to avoid any irregularities, however, temperature and voltage data are only used from the last full current oscillation out of the 5 simulated for any given frequency.

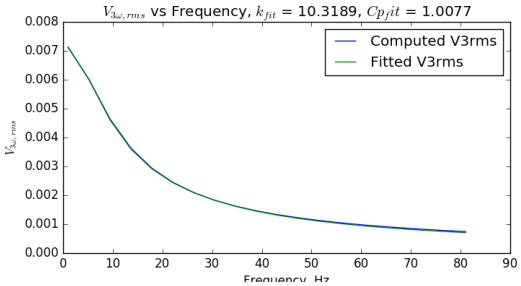

Figure 2: 3ω V_{rms} vs current frequency with 0 ambient temperature

For 0 ambient temperature, as in Fig. 2, it is expected that the radiative component is very small. This results in the apparent thermal conductivity being quite close to the actual value, but slightly higher due to the excess heat transfer out of the sample. The difference here from the estimation presented by Lu et al., is that the error analysis linearized radiative heat transfer for small variations in temperature from ambient, while this finite volume method preserves the full temperature to the fourth relation. This nonlinearity may also be used to help explain why the apparent specific heat is close to but not exactly 1.

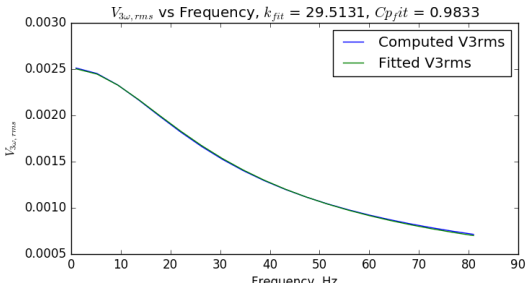

Figure 3: 3ω V_{rms} vs current frequency with 275 K ambient temperature

For 275 K ambient temperature, as in Fig. 3, a much higher apparent thermal conductivity is observed in addition to a relatively unchanged specific heat. Again, this slight variation from the expected for specific heat may be attributed to the nonlinearity of true radiation, or perhaps numerical error, but the specific heat is still relatively insensitive to change. According to Lu, the expected change in apparent thermal conductivity behaves according to: $\kappa_{ap} = (1 + g\gamma)\kappa$, where

$$g = 4\epsilon\sigma \left[T^3 + 4T^2T_0 + 6TT_0 + 4T_0^3\right] \tag{14}$$

was the coefficient of linear temperature variation due to radiation. Approximating this with $T \approx 0.4$ results in $g \approx 190$ and $\kappa_{ap} = 29.17$. This is only $\sim 1\%$ off from the simulation value, which shows very good agreement.

CONCLUSIONS

The 3ω method as presented by Lu provides a robust method for simultaneously determining the thermal conductivity and specific heat of a material, provided that certain assumptions regarding the dimensionality of heat transfer are satisfied. In an experimental setting, these assumptions are readily verifiable and potential sources of error such as radial heat loss through convection or radiation are either easily minimizable or defendably negligible. Even in the unlikelihood that these contamination sources are unavoidably large, the specific heat measurement is shown to retain its accuracy, even though the apparent thermal conductivity may become incorrectly large. Furthermore, the high and low frequency limits of this analytical solution are shown to be consistent with those obtained by Cahill [9] and Holland [10].

A computational model of this measurement method was then constructed with exactly known material properties to study the predictability of the model under a scenario with significant radiative heat transfer. The resulting specific heat was not found to significantly change from the exact value, as expected, and the calculated apparent thermal conductivity was very well predicted.

Future work may involve the explicit application of this method to different sample geometries, or perhaps the influence of imperfect boundary conditions.

References

[1] L. Lu, W. Yi, and D. L. Zhang. "3ω method for specific heat and thermal conductivity measurements". In: *Review of Scientific Instruments* 72.7 (2001), pp. 2996–3003. DOI: http://dx.doi.org/10.1063/1.1378340.

[2] Qin-Yi Li, Masahiro Narasaki, and Koji Takahashi. "Temperature-dependent specific heat of suspended platinum nanofilms at 80-380 K". In: *Chinese Physics B* 25.11 (2016). DOI: https://doi.org/10.1088/1674-1056/25/11/114401.

[3] Gang Meng et al. "Nanoscale Thermal Management of Single SnO_2 Nanowire: pico-Joule Energy Consumed Molecular Sensor". In: *ACS Sensors* 1.8 (2016), pp. 997–1002. DOI: http://dx.doi.org/10.1021/acssensors.6b00364.

[4] Lin Qiu et al. "Functionalization and densification of inter-bundle interfaces for improvement in electrical and thermal transport of carbon nanotube fibers". In: *Carbon* 105 (2016), pp. 248–259. DOI: http://dx.doi.org/10.1016/j.carbon.2016.04.043.

[5] Gergo P. Szakmany et al. "Evaluating the Frequency Response of Nanoscale Thermocouples Using Temperature Oscillations in Nanoscale Heaters". In: *IEEE Transactions on Nanotechnology* 15.4 (2016), pp. 567–573. DOI: http://dx.doi.org/10.1109/TNANO.2016.2556321.

[6] O. M. Corbino. In: *Phys. Z.* 11 (1910), p. 413. DOI: https://doi.org/PHZTAO.

[7] J. E. Lorrimer, J. T. McMullan, and D. G. Walmsley. In: *Physics Education* 11.1 (1976), pp. 42–44. DOI: https://doi.org/10.1088/0031-9120/11/1/004.

[8] S. Reigel and G. Weber. In: *Journal of Physics E: Scientific Instruments* 19.10 (1986), pp. 790–791. DOI: https://doi.org/10.1088/0022-3735/19/10/006.

[9] D.G. Cahill. "Thermal conductivity measurement from 30 to 750 K: the 3ω method". In: *Review of Scientific Instruments* 61 (1990), pp. 802–808. DOI: 10.1063/1.1141498.

[10] L. R. Holland. "Physical Properties of Titanium. III. The Specific Heat". In: *Journal of Applied Physics* 34.8 (1963), pp. 2350–2357. DOI: http://dx.doi.org/10.1063/1.1702745.